

# Hypoxia-induced autophagy contributes to the invasion of salivary adenoid cystic carcinoma through the HIF-1 $\alpha$ /BNIP3 signaling pathway

HAIWEI WU\*, SHENGYUN HUANG\*, ZHANWEI CHEN\*, WENLEI LIU,  
XIAOQING ZHOU and DONGSHENG ZHANG

Department of Oral and Maxillofacial Surgery, Shandong Provincial Hospital Affiliated to Shandong University,  
Jinan, Shandong 250021, P.R. China

Received October 30, 2014; Accepted July 21, 2015

DOI: 10.3892/mmr.2015.4255

**Abstract.** Adenoid cystic carcinoma (ACC) is one of the most common types of salivary gland malignancy in the head and neck, and its aggressive ability to invade and metastasize is an important reason for its poor survival rates. Our previous investigations confirmed that autophagy-associated gene expression is closely associated with the occurrence and development of ACC. On this basis, the present study further investigated hypoxia-induced autophagy and its role in tumor invasion. Cobalt chloride (CoCl<sub>2</sub>) was used to mimic hypoxia. The results of the present study indicated that autophagosome formation and upregulation of autophagy-associated microtubule-associated protein 1 light chain 3 and Beclin 1 were observed in ACC-M cells in response to CoCl<sub>2</sub>. The hypoxia-inducible factor 1 $\alpha$ /B cell lymphoma 2/adenovirus E1B 19K-interacting protein 3 signaling pathway was involved in hypoxia-induced autophagy in ACC. Furthermore, inhibition of autophagy by chloroquine markedly attenuated the tumor invasion induced by mimetic hypoxia in ACC. These results suggested that hypoxia-induced autophagy may serve as a potential target for the future treatment of ACC.

## Introduction

Adenoid cystic carcinoma (ACC) is an aggressive type of malignancy, which develops in major and minor salivary glands and rarely in other sites. ACC accounts for ~10%

of all neoplasia of the salivary glands, 22% of all salivary gland malignancies, and ~1% of all head and neck malignancies (1-3). A hallmark of ACC is its aggressive ability to invade and metastasize. It is currently accepted that local disease requires treatment by local radical excision and postoperative radiotherapy, while chemotherapy may have a limited benefit for advanced ACC (4,5). Tumor cells are characterized by high proliferation rates and demand for oxygen and nutrients. However, the abnormal structure and function of the vascular network leads to inadequate blood flow and fails to satisfy tumor cell demand for oxygen and nutrients, which contributes to the formation of a hypoxic microenvironment (4). It is widely accepted that hypoxia is intricately associated with tumor aggressiveness, angiogenesis, increased rates of recurrence and chemotherapy resistance (6).

Hypoxia-inducible factor-1 (HIF-1) is an important heterodimeric transcription factor composed of a labile HIF-1 $\alpha$  subunit and a stable HIF-1 $\beta$  subunit (7). Under normoxic conditions, HIF-1 $\alpha$  is degraded proteasomally; whereas under hypoxic conditions, HIF-1 $\alpha$  is stabilized and moves to the nucleus where it freely forms a complex with HIF-1 $\beta$ , which in turn binds to hypoxia response elements and induces the transcription of several genes, including >60 genes activated by HIF-1 (8,9). The expression of HIF-1 $\alpha$  has been detected in ordinary and transformed ACC, and occasionally in normal salivary tissues adjacent to the tumor (10). Previously, HIF-2 $\alpha$ , one of the three homologues of the HIF $\alpha$  subunit, has also been observed in ACC tissues, and correlated with invasion and metastasis (11). On the basis of these findings, HIFs may be important in the aggressive behavior of ACC.

Autophagy is an important intracellular process involved in the degradation and recycling of cytosolic material, which is essential for the maintenance of cellular biosynthesis (12). Accumulating evidence supports a controversial role for autophagy in cancer, as autophagy enables tumor cells to tolerate adverse stress conditions, including hypoxia, and autophagy may protect cells through damage mitigation, which may limit tumorigenesis (13). Our previous study investigated 79 patients with head and neck ACC, and observed the expression levels of autophagy-associated protein 1 light chain 3 (LC3) and Beclin 1. The results indicated that LC3 and

---

*Correspondence to:* Professor Dongsheng Zhang, Department of Oral and Maxillofacial Surgery, Shandong Provincial Hospital Affiliated to Shandong University, 324 Jingwu Road, Jinan, Shandong 250021, P.R. China  
E-mail: ds63zhang@sdu.edu.cn

\*Contributed equally

**Key words:** autophagy, adenoid cystic carcinoma, hypoxia, hypoxia-inducible factor 1 $\alpha$ , tumor invasion

Beclin 1 may be important in the tumorigenesis of ACC (14). Furthermore, inhibition of autophagy enhanced chemotherapy efficacy in ACC (15), and these results were concordant with those of and Ma *et al* (16). Therefore, further studies on autophagy and a better understanding of the role of autophagy in ACC is essential for future developments in its treatment.

Previous studies have uncovered several associations between hypoxia and the induction of autophagy (12,13). However, the molecular mechanism underlying hypoxia-induced autophagy in ACC remains to be elucidated. Considering the correlation between hypoxia and tumor invasion in ACC (11), whether hypoxia-induced autophagy is associated with tumor invasion in ACC also remains to be elucidated. In the present study, ACC-M cell lines were treated with the hypoxia mimetic cobalt chloride ( $\text{CoCl}_2$ ) to investigate the levels of hypoxia mimetic-induced autophagy in salivary ACC cells and its effects on tumor invasion.

## Materials and methods

**Chemical reagents and antibodies.**  $\text{CoCl}_2$ , chloroquine (an inhibitor of autophagy) and antibodies targeting LC3B were purchased from Sigma-Aldrich (St. Louis, MO, USA). Antibodies targeting HIF-1 $\alpha$  and B cell lymphoma 2 (Bcl-2)/adenovirus E1B 19K-interacting protein 3 (BNIP3) were purchased from Santa Cruz Biotechnology, Inc. (Dallas, TX, USA). Antibodies targeting Beclin 1 and GAPDH were purchased from Abcam (Cambridge, MA, USA).

**Cell culture.** The ACC-M cell lines were obtained from Professor Wantao Chen (Department of Oral and Maxillofacial Surgery, Ninth People's Hospital, College of Stomatology, Shanghai Jiao Tong University, Shanghai, China), and were maintained in culture with Dulbecco's modified Eagle's medium (Invitrogen Life Technologies, Carlsbad, CA, USA) supplemented with 10% fetal bovine serum (Invitrogen Life Technologies) in a humidified atmosphere containing 5%  $\text{CO}_2$  at 37°C. To induce a hypoxic environment, the cells were plated on a 35 mm dish and, after 24 h, were cultured in medium supplemented with  $\text{CoCl}_2$  in an atmosphere containing 5%  $\text{CO}_2$  at 37°C.

**Cell viability assay.** Cell viability assays were performed using an MTT assay (Sigma-Aldrich). Briefly, the cells were plated into 96-well plates at a density of  $1 \times 10^4$  cells/well. Following overnight incubation, the cells were treated with the indicated concentrations of  $\text{CoCl}_2$  (50, 100, 150, 200, 250, 300, 500 and 1,000  $\mu\text{mol/l}$ ) for 24 h. A total of 20  $\mu\text{l}$  MTT solution (5 mg/ml) was subsequently added to each well and incubated for 4 h at 37°C. Blotting nutrient solution and 150  $\mu\text{l}$  dimethyl sulfoxide (DMSO; Sigma-Aldrich) were placed in each well. Following agitation for 10 min, the absorption value of each well was measured at 570 nm using an enzyme-linked immune detector (Softmax PRO M2, Molecular Devices, Sunnyvale, CA, USA). Cell viability was expressed as the percentage of viable cells relative to the untreated cells. All experiments were performed in triplicate.

**Transmission electron microscopy (TEM).** TEM was performed, as previously described (15). The ACC-M cells

( $1 \times 10^6$ ) were incubated with DMSO (control) and 200  $\mu\text{M}$   $\text{CoCl}_2$  for 24 h at 37°C. The cells were then fixed with 2% glutaraldehyde (Beijing Chemical Industry Group, Co., Ltd., Beijing, China) in 0.1 M Sorensen buffer (pH 7.3; Beijing Chemical Industry Group, Co., Ltd.) for 1 h at 4°C, and post-fixed in 1% osmium tetroxide (Beijing Chemical Industry Group, Co., Ltd.) in 0.1 M cacodylate buffer (Beijing Chemical Industry Group, Co., Ltd.) for 1 h at room temperature. The specimens were dehydrated through a graded series of ethanol (30-90%), and embedded in Epon (Beijing Chemical Industry Group, Co., Ltd.). Following staining with 2% uranyl acetate (Beijing Chemical Industry Group, Co., Ltd.), thin sections (50-70 nm) were prepared with a UC7 microtome (Leica, Wetzlar, Germany). were observed using a JEM-1200EX Transmission Electron Microscope (JEOL, Ltd., Tokyo, Japan).

**Immunofluorescence staining.** A total of  $2 \times 10^5$  ACC-M cells were grown on coverslips in 6 cm dishes, allowed to attach by overnight incubation at 37°C, and then cultured with DMSO (control) or 200  $\mu\text{M}$   $\text{CoCl}_2$  for 24 h. At the end of treatment, the cells were washed with phosphate-buffered saline (PBS), fixed with 4% paraformaldehyde (Beijing ComWin Biotech Co., Ltd., Beijing, China); for 20 min, washed twice with PBS for 5 min and permeabilized with 0.5% Triton X-100 (Beijing ComWin Biotech Co., Ltd.) for 10 min. Following washing with PBS, the cells were incubated with primary antibody at 4°C overnight. For LC3 localization detection, the cells were incubated with rabbit anti-LC3B antibody (1:50 diluted in 5% non-fat milk, polyclonal, cat. no. L8918); fluorescein isothiocyanate (FITC)-conjugated goat anti-rabbit immunoglobulin (Ig) G (1:50 diluted in 5% non-fat milk, cat. no. cw0114) (both from Beijing ComWin Biotech Co., Ltd., Beijing, China) for 1 h at 4°C. The nuclei were then counterstained with DAPI (Beijing ComWin Biotech Co., Ltd.); for 7 min, and observed under a fluorescence microscope (TE2000; Nikon Corporation, Tokyo, Japan). In order to further identify the hypoxia-induced autophagy pathway, double immunofluorescence labeling was performed by simultaneous incubation of mouse anti-BNIP3 (1:100 diluted in 5% non-fat milk, monoclonal, cat. no. sc56167); rabbit anti-HIF-1 $\alpha$  (1:100 diluted in 5% non-fat milk, polyclonal, cat. no. sc10790); tetramethylrhodamine-conjugated goat anti-mouse IgG (1:50 diluted in 5% non-fat milk, cat. no. cw0167) (both from Beijing ComWin Biotech Co., Ltd., Beijing, China) for 1 h at 37°C. The subsequent staining procedure was performed, as described for the LC3B-positive cells.

**Reverse transcription-quantitative polymerase chain reaction (RT-qPCR).** Total RNA was extracted from cells using TRIzol reagent (Takara Biotechnology, Co., Ltd., Dalian, China), according to the manufacturer's instructions. Reverse transcription of 1  $\mu\text{g}$  total RNA was performed with the PrimeScript™ RT reagent kit (Takara Biotechnology, Co., Ltd.) with gDNA Eraser (Takara Biotechnology, Co., Ltd.), according to the manufacturer's instructions. The total 20  $\mu\text{l}$  reacting solution included 10  $\mu\text{l}$  SYBR® Green mix (Takara Biotechnology, Co., Ltd.), 0.8  $\mu\text{l}$  PCR forward primer, 0.8  $\mu\text{l}$  PCR reverse primer, 0.4  $\mu\text{l}$  ROX reference dye, 2  $\mu\text{l}$  cDNA and 6  $\mu\text{l}$   $\text{dH}_2\text{O}$ . The ACC-M cells were detached and homogenized using TRIzol® (Takara Biotechnology Co., Ltd.) and total RNA was extracted. RT-qPCR was performed using a Roche

Light Cycler 480 (Roche Diagnostics GmbH, Mannheim, Germany) in a total volume of 20  $\mu$ l reacting solution. The following gene-specific primers were used: HIF-1 $\alpha$  forward, 5'-CATCAGTTGCCACTTCCACATAA-3' and reverse, 5'-GAGAACCATAACAAAACCATCCAAG-3'; BNIP3 forward, 5'-GCTTCTGAAACAGATACCCATAGCA-3' and reverse, 5'-CGACTTGACCAATCCCATATCC-3'; LC3B forward, 5'-AAACGCATTTGCCATCACA-3' and reverse, 5'-GGACCTTCAGCAGTTTACAGTCAG-3'; and  $\beta$ -actin forward, 5'-TGGCACCCAGCACAATGAA-3' and reverse, 5'-CTAAGTCATAGTCCGCCTAGAAGCA-3' (Takara Biotechnology Co., Ltd.). The cycling conditions were identical for all primers. SYBR<sup>®</sup> Green Mix (Takara Biotechnology Co., Ltd.) was used to determine the abundance of mRNA, and the mRNA levels were calculated relative to those of  $\beta$ -actin. The reaction conditions were as follows: Stage 1, one cycle as 95°C for 30 sec; stage 2, 40 cycles at 95°C for 5 sec, and 60°C for 34 sec; followed by a dissociation stage (95°C for 15 sec; 60°C for 1 min; 95°C for 15 sec). The comparative threshold cycle ( $2^{-\Delta\Delta CT}$ ) method was used to quantify the mRNA expression levels of these genes.

**Western blot analysis.** To extract the total protein of the cells, the treated cells were washed three times with ice-cold PBS, and then lysed in lysis buffer (RAPA:phenylmethylsulfonyl fluoride, 100:1; Shennong Bocai Biotechnology Co., Ltd., Shanghai, China). A bicinchoninic acid protein assay kit (Shennong Bocai Biotechnology Co., Ltd.) was used to quantify the total protein content, expressed in mg/ml. Samples containing equal quantities of protein were resolved using 10-15% SDS-PAGE gels (Shennong Bocai Biotechnology Co., Ltd.) and transferred onto polyvinylidene fluoride membranes (Shennong Bocai Biotechnology Co., Ltd.). The membranes were then incubated with primary antibodies targeting HIF-1 $\alpha$  (1:750), BNIP3 (1:1,000), LC3B (1:1,000) and Beclin 1 (1:1,000) overnight. The membranes were subsequently incubated with peroxidase-conjugated secondary antibodies for 60 min. Protein bands incubated with enhanced chemiluminescence reagents (Shennong Bocai Biotechnology Co., Ltd.) were visualized using an Alpha Imager 2200 system (Alpha Innotech Corporation, San Leandro, CA, USA). To ensure equal protein loading, each membrane was stripped and reprobed with anti-GAPDH antibody (1:1,000). GAPDH was used as a control for protein level quantification. The band density was quantified by the Quantity One image processing program, version 4.62 (Bio-Rad Laboratories, Inc., Hercules, CA, USA).

**Cell invasion assay.** An invasion assay was performed using a BD BioCoat Growth Factor Reduced Matrigel Invasion Chamber (BD Biosciences, San Jose, CA, USA), according to the manufacturer's instructions. An equivalent number of cells ( $5 \times 10^4$ /well) was resuspended in serum-free medium, with or without CoCl<sub>2</sub> (200  $\mu$ M), and plated in the upper insert. To further examine the effects of autophagy inhibition on invasion under hypoxia, another group of cells were incubated in the presence or absence of chloroquine (CQ; 10 and 20  $\mu$ M; Sigma-Aldrich) with 200  $\mu$ M CoCl<sub>2</sub>. The insert was then placed inside a 24-well plate. The cells were incubated for 24 h at 37°C, following which the upper surface of the membrane in each insert was gently wiped with a

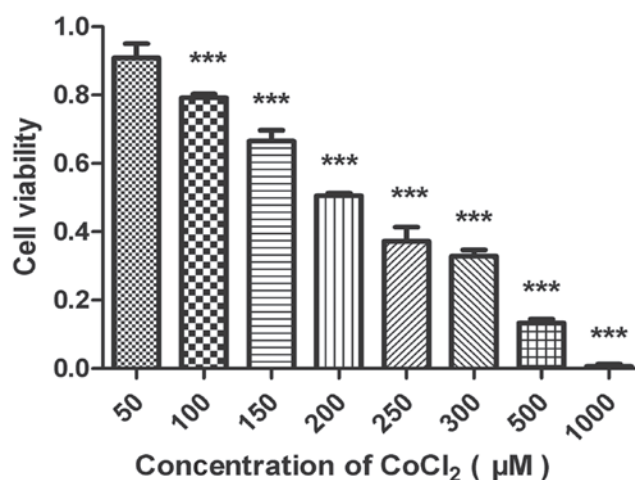


Figure 1. Effects of CoCl<sub>2</sub> on ACC-M cell viability. The ACC-M cells were cultured with various concentrations (50-1000  $\mu$ M) of CoCl<sub>2</sub> for 24 h and cell viability was analyzed using an MTT assay. The viability of control cells in the absence of CoCl<sub>2</sub> treatment was defined as 100%, compared with the control group (\*\*P<0.001 vs. 50  $\mu$ l CoCl<sub>2</sub> treatment group). The data are presented as the mean  $\pm$  standard error of the mean of three independent experiments. ACC, adenoid cystic carcinoma; CoCl<sub>2</sub>, cobalt chloride.

cotton swab to remove all non-invading cells. The cells on the under surface were fixed with 4% paraformaldehyde for 15 min. The insert was subsequently placed in 0.1% crystal violet (Beijing Chemical Industry Group, Co., Ltd.) to stain the cells. The numbers of cells in seven randomly-selected fields of each filter were estimated by manual counting, and each experiment was performed independently at least three times. Leica-DM4000B microscope.

**Statistical analysis.** The data are expressed as the mean  $\pm$  standard error of the mean of at least three independent experiments. Statistical comparisons between groups were performed using two-tailed Student's *t*-test. Statistical analysis was performed using SPSS 15.0 (SPSS, Inc., Chicago, IL, USA). P<0.05 was considered to indicate a statistically significant difference.

## Results

**Cell viability assay.** In the present study, ACC-M cells were treated with hypoxia mimetic CoCl<sub>2</sub>. An MTT assay was used to quantify the viability of the ACC-M cells treated with CoCl<sub>2</sub>. As shown in Fig. 1, CoCl<sub>2</sub> markedly reduced the viability of the ACC-M cells in a clear dose-dependent manner. According to the experimental data, the 50% inhibitory concentration of CoCl<sub>2</sub> in the culture system was  $\sim$ 200  $\mu$ mol/l.

**Autophagosome formation in ACC-M cells in response to CoCl<sub>2</sub>.** Our previous study reported that autophagy-associated protein expression was observed in ACC tissue samples (14). In order to examine whether hypoxia induced autophagy in the ACC-M cells, the present study used morphological analyses. LC3-II is conjugated with phosphatidylethanolamine and is present on isolated membranes and autophagosomes. Although LC3 has several homologs in mammals, LC3B is most commonly used for autophagy assays (17). Therefore, immunostaining with LC3B was used in the present study to observe the formation



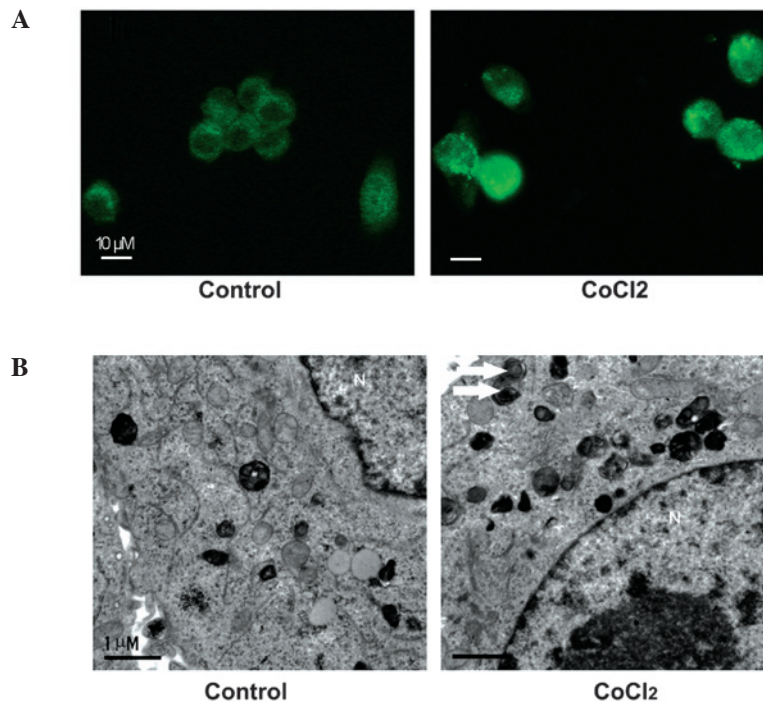


Figure 2.  $\text{CoCl}_2$  induces autophagosome formation in ACC-M cells. ACC-M cells were cultured with dimethyl sulfoxide (control) or  $200 \mu\text{M}$   $\text{CoCl}_2$  for 24 h. (A) Levels of LC3 were measured using a fluorescence microscope. Autophagosome formation was visualized in the LC3-punctuated cells (scale bar,  $10 \mu\text{m}$ ). (B) Numerous autophagosomes or lysosomes containing segregation and degradation of organelles were observed in the  $\text{CoCl}_2$  groups. Magnification,  $\times 10,000$ . Short white arrows are representative of autophagosome-like structures consisting of double membranes (scale bar,  $1 \mu\text{m}$ ).  $\text{CoCl}_2$ , cobalt chloride; LC3, autophagy-associated protein 1 light chain 3; ACC, adenoid cystic carcinoma.

of autophagosomes. Increased numbers of cytoplasmic puncta tethered with LC3B were present in the  $\text{CoCl}_2$ -treated ACC-M cells, compared with the untreated cells (Fig. 2A). These results suggested the formation of autophagosomes in the ACC-M cells. TEM was used for further confirmation. Numerous autophagosome-like structures consisting of double membranes were observed in the  $\text{CoCl}_2$ -treated ACC-M cells, compared with untreated cells, which was indicative of autophagosome formation (Fig. 2B). In conclusion, these results indicated that the  $\text{CoCl}_2$  mimetic hypoxia induced the formation of autophagosomes in the ACC-M cells.

**Involvement of the HIF-1 $\alpha$ /BNIP3 signaling pathway in  $\text{CoCl}_2$ -induced autophagy in ACC-M cells.** Increasing evidence has demonstrated that the HIF-1-dependent signaling pathway is important in hypoxia-induced autophagy (18). In addition, BNIP3, a downstream gene regulated by HIF-1, has been demonstrated to be essential for the HIF-1-dependent signaling pathway in several cell lines (19,20). The present study demonstrated the involvement of the HIF-1 $\alpha$ /BNIP3 signaling pathway in  $\text{CoCl}_2$ -induced autophagy in ACC. As shown in Fig. 3A, treatment of the ACC-M cells with  $200 \mu\text{mol/l}$   $\text{CoCl}_2$  resulted in a marked increase in the protein expression levels of HIF-1 $\alpha$  and BNIP3 at different time-points. Double immunofluorescence labeling of HIF-1 $\alpha$  and BNIP3 confirmed the expression of HIF-1 $\alpha$  in the nucleus, and expression of BNIP3 in the cytoplasm (Fig. 3D), whereas fluorescence in the untreated cells was limited (data not shown). As shown in Fig. 3C, the mRNA expression levels of HIF-1 $\alpha$  were not affected by  $\text{CoCl}_2$  treatment; however, following 24 h of treatment with  $\text{CoCl}_2$ , a ~6-fold increase in the mRNA

expression of BNIP3 was observed ( $P < 0.001$ ). With regards to autophagy-associated gene expression in ACC, a marked increase in the expression of LC3B-II was observed, however, minimal change was detected in the expression of LC3B-I (Fig. 3B). The mRNA expression levels of LC3B were also significantly increased following 24 h of treatment with  $\text{CoCl}_2$  ( $P < 0.001$ ; Fig. 3C). In addition, an increase in the expression of Beclin 1 was detected using western blot analysis (Fig. 3B). These results suggested that the mimetic hypoxia induced autophagy in the ACC-M cells and that the HIF-1 $\alpha$ /BNIP3 signaling pathway is essential for hypoxia-induced autophagy in ACC.

**Inhibition of autophagy attenuates tumor invasion induced by hypoxia in ACC-M cells.** In the present study, a cell invasion assay was used to determine the effect of mimetic hypoxia on tumor invasion. Compared with the untreated cells, invasive cell numbers under mimetic hypoxia were significantly increased ( $P < 0.001$ ; Fig. 4A and B). To further examine the role of hypoxia-induced autophagy in tumor invasion in ACC, the ACC-M cells were treated with or without CQ ( $10 \mu\text{M}$  and  $20 \mu\text{M}$ ) under mimetic hypoxia. The number of invading ACC-M cells under mimetic hypoxia was markedly reduced 24 h after CQ treatment (Fig. 4C and D), and higher concentrations of CQ had an increased effect on the inhibition of tumor invasion, compared with lower concentrations ( $P < 0.001$ ).

## Discussion

Our previous study reported that autophagy may be important in the tumorigenesis of ACC (14). Considering the

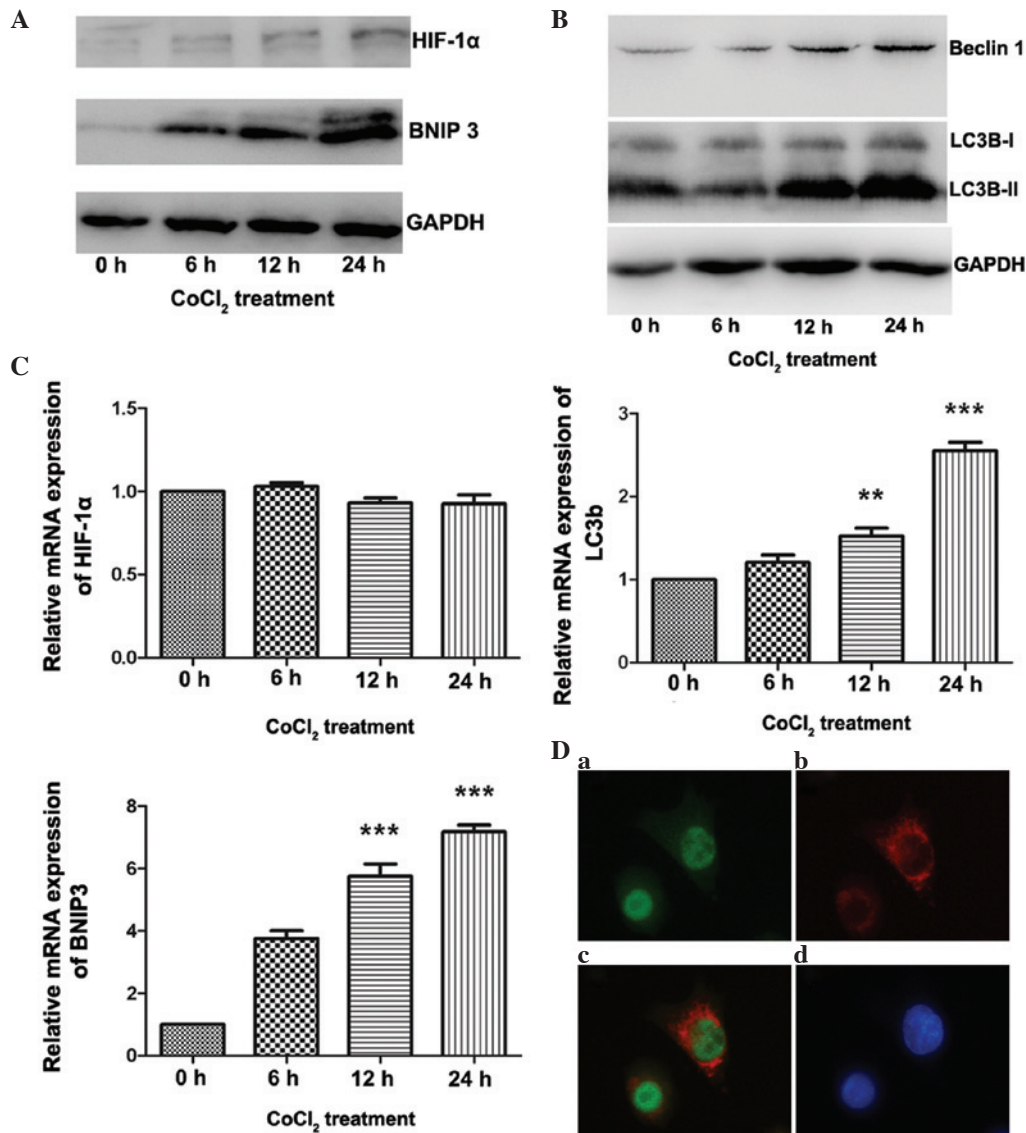


Figure 3. HIF-1α/BNIP3 pathway is activated in ACC-M cells treated with CoCl<sub>2</sub>. The ACC-M cells were cultured with 200 μM CoCl<sub>2</sub> for the indicated time-periods. Untreated cells (0 h group) served as a control. (A) Variations in the protein expression levels of HIF-1α and BNIP3 were compared using western blotting, with GAPDH as an internal control. (B) Expression levels of autophagy-associated proteins were increased in the ACC-M cells treated with CoCl<sub>2</sub>. The ACC-M cells were cultured with 200 μM CoCl<sub>2</sub> for the indicated time-periods. Untreated cells (0 h group) served as a control. Variations in the protein expression levels of Beclin 1 and LC3 were compared using western blotting, with GAPDH as an internal control. (C) Variations in the mRNA expression levels of HIF-1α, BNIP3 and Beclin1 were examined using reverse transcription-quantitative polymerase chain reaction. The ACC-M cells were cultured with 200 μM CoCl<sub>2</sub> for the indicated time-periods. Untreated cells (0 h group) served as a control. \*P<0.05, \*\*P<0.01 and \*\*\*P<0.001, vs. control group. The data are presented as the mean ± standard error of the mean of three independent experiments with duplicates. (D) Double immunofluorescent staining for HIF-1α and BNIP3 in the ACC-M cells treated with CoCl<sub>2</sub>. (a) HIF-1α, (b) BNIP3, (c) merged signals, (d) DAPI staining in the nucleus. The staining was observed by fluorescence microscopy; magnification, x400. HIF-1α, hypoxia-inducible factor 1α; BNIP3, B cell lymphoma 2/adenovirus E1B 19K-interacting protein 3; CoCl<sub>2</sub>, cobalt chloride; ACC, adenoid cystic carcinoma.

ubiquitous existence of hypoxia in ACC (10,11), the present study investigated whether hypoxia induces autophagy in ACC, and investigated its role in tumor invasion. To the best of our knowledge, the present study is the first to report the effects of CoCl<sub>2</sub> on autophagy in ACC. In the present study, mimetic hypoxia induced by CoCl<sub>2</sub> markedly upregulated the formation of autophagosome, and the expression levels of autophagy-associated genes. In addition, the results demonstrated that HIF-1α and its target gene, BNIP3, are important in hypoxia-induced autophagy in ACC. Exposure to CoCl<sub>2</sub> increased the number of invading cells, and inhibition of autophagy attenuated hypoxia-induced tumor invasion in ACC-M cells.

Hypoxia develops in tumors due to incomplete vascular supply and increasing demand for oxygen, compared with normal tissues (4). Accumulating evidence suggests that hypoxia exists in the majority of types of head and neck cancer and is indicated as an important negative factor (4). CoCl<sub>2</sub> has been widely used to mimic hypoxia, which can disturb the degradation of HIF-1α and lead to its overexpression (21). Previous studies have demonstrated that CoCl<sub>2</sub> induces apoptosis and autophagic cell death in several cell types, including human periodontal ligament cells (22) and neuroblastoma cells (23), and increasing CoCl<sub>2</sub> doses affects cell viability in a dose-dependent manner (24), which was also demonstrated in in ACC-M cells in the present study.

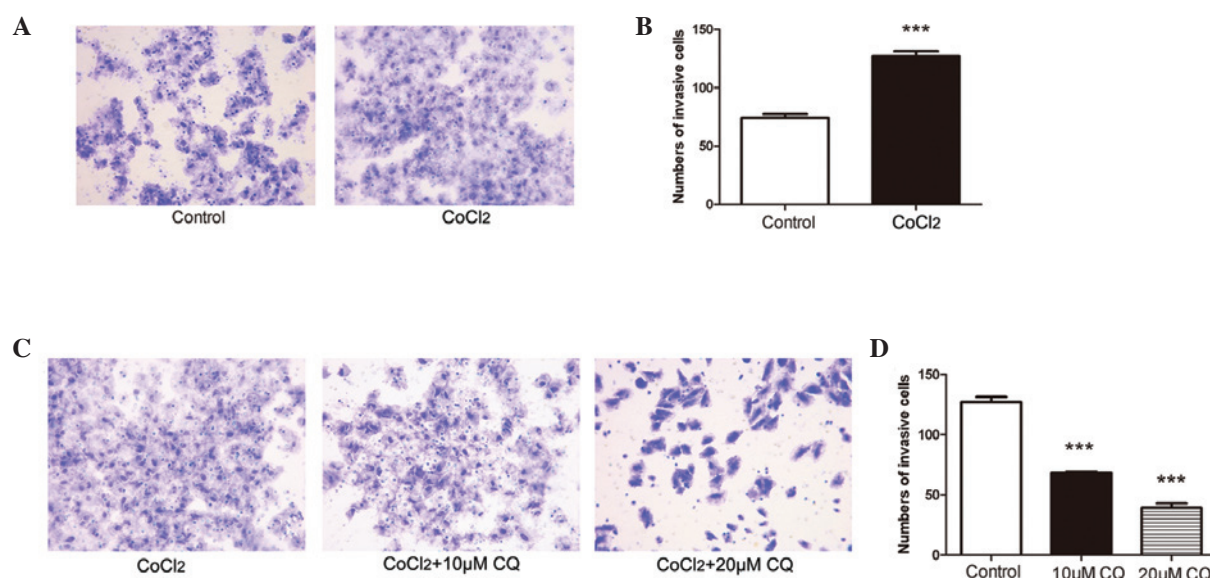


Figure 4. Inhibition of autophagy by CQ attenuates tumor invasion induced by hypoxia in ACC-M cells. (A and B) Number of invading ACC-M cells treated with or without 200  $\mu$ M CoCl<sub>2</sub>. Invasive ACC-M cells with or without 200  $\mu$ M CoCl<sub>2</sub> were stained with 0.1% crystal violet. Magnification,  $\times 100$ . Cells cultured in complete medium served as a control. All data are representative of three independent experiments and presented as the mean  $\pm$  SEM (\*\*\* $P$ <0.001, vs. control group). (C and D) Number of invading ACC-M cells treated with 200  $\mu$ M CoCl<sub>2</sub> in the absence or presence of CQ (10  $\mu$ M and 20  $\mu$ M). Invasive ACC-M cells under 200  $\mu$ M CoCl<sub>2</sub> treatment in the absence or presence of CQ (10  $\mu$ M and 20  $\mu$ M) were stained with 0.1% crystal violet. Magnification,  $\times 100$ . Cells cultured in 200  $\mu$ M CoCl<sub>2</sub> without CQ served as a control. All data are representative of three independent experiments and presented as the mean  $\pm$  SEM (\*\*\* $P$ <0.001, vs. control group). SEM, standard error of the mean; CQ, chloroquine; CoCl<sub>2</sub>, cobalt chloride; ACC, adenoid cystic carcinoma.

As a transcriptional factor, HIF-1 $\alpha$  moves to the nucleus and forms a complex with HIF-1 $\beta$ , where it induces the transcription of numerous genes, including BNIP3 (7-9). BNIP3 is a BH3-only Bcl-2 family member regulated by HIF-1, and has been identified as one of the most prominent hypoxia-responsive genes (25). Under hypoxic conditions, the expression levels of BNIP3 and BNIP3L are elevated and contribute to hypoxia-induced cell death (25). Vengellur *et al* (26) demonstrated that the expression of BNIP3 is HIF-1 $\alpha$ -dependent, and CoCl<sub>2</sub> induces their expression in a time- and dose-dependent manner in mouse embryonic fibroblasts (26). Concordant with these studies, the protein and mRNA expression levels of BNIP3 were elevated following CoCl<sub>2</sub> treatment in a time-dependent manner in the present study.

Autophagy is a lysosomal degradation pathway, which involves the degradation and recycling of cytoplasm material. Autophagy is characterized by at least four fundamental steps: Induction; entrapment of organelles and cytoplasm in double-membrane vesicles, termed autophagosomes; autophagosome docking and fusion with the lysosome or vacuole; and autophagic body degradation (27). Hypoxia is able to rapidly induce autophagy in an HIF-1-dependent pathway. By investigating HIF-knockdown cells, Bohensky *et al* (28) demonstrated that HIF-1 modulates the induction of autophagic proteins by regulating the association between Bcl-2 and Beclin 1. In a previous study on the functional and physical interactions between Bcl-2 and Beclin 1, the BH3 domain was demonstrated to be involved in autophagy (29,30). Consequently, members of the BH3-only subfamily, including BNIP3, are under further investigation. Bellot *et al* (19) demonstrated that the atypical BH3 domains of hypoxia-induced BNIP3/BNIP3L induce autophagy by disrupting the Bcl-2/Beclin 1 complex without inducing cell death (19). These findings suggest that

the HIF-1 $\alpha$ /BNIP3 signaling pathway may be important in mimetic hypoxia-induced autophagy in ACC. The results of the present study demonstrated that exposure to CoCl<sub>2</sub> resulted in overexpression of HIF-1 and activation of BNIP3, as well as upregulation of autophagosome formation and in the expression levels of Beclin 1 and LC3-II. Therefore, the results of the present study demonstrated that mimetic hypoxia by CoCl<sub>2</sub> was able to induce autophagy via the HIF-1 $\alpha$ /BNIP3 signaling pathway in ACC.

By affecting the degradation of the basement membrane and extracellular matrix (ECM), modulation of cell adhesion molecules and cell migration, hypoxia is able to promote tumor invasion and metastasis (31). In ACC-M cells in the present study, exposure to mimetic hypoxia markedly increased tumor invasion. A previous study demonstrated that hypoxia-induced autophagic stroma, including fibroblasts and ECM, are important in tumor invasion and metastasis via paracrine secretion (27).

Whether autophagy of tumor cells is involved in the process of invasion and metastasis remains to be fully elucidated, therefore, investigations to examine the effects of autophagy on tumor invasion are required. Macintosh *et al* (32) investigated the role of autophagy in tumor cell invasion using a three-dimensional (3D) organotypic model. The results demonstrated that inhibition of autophagy by shAtg12 failed to affect cell migration, but impaired tumor invasion in the 3D organotypic model (32). These results are concordant with the findings of the present study, which demonstrated that inhibition of autophagy attenuated hypoxia-induced tumor invasion in ACC-M cells. To further investigate the molecular mechanism underlying the role of autophagy in tumor invasion, Li *et al* (33) reported that autophagy promoted hepatocellular carcinoma cell invasion through activation



of transforming growth factor  $\beta$ /Smad3 signaling during starvation. Yamanaka-Tatematsu *et al* (34) demonstrated that the autophagy induced by  $\text{CoCl}_2$  treatment increases tumor invasion through supplementation of adenosine triphosphate (ATP). These findings suggested that recruitment of ATP supplied by autophagy may be vital to tumor invasion. These results are concordant with those of a previous report that demonstrated that ATP induces the release of matrix metalloproteinase 9 to support invasion (35). Indelicato *et al* (36) reported that activation of autophagy also inhibits tumor invasion via the induction of HIF-1 $\alpha$  degradation by autophagy. However, whether inhibition or activation of autophagy attenuates tumor invasion remains to be elucidated. In the present study, CQ was selected as an autophagic inhibitor. CQ and hydroxyl-CQ are the only autophagic inhibitors used in clinical trials at present (12). The results of the present study indicated that combining traditional treatment with autophagic target therapy may be efficient in suppressing tumor invasion of ACC. However, identifying the regulatory mechanism underlying autophagy in tumor invasion is important in order for autophagy to be targeted in future treatment.

In conclusion, the results of the present study revealed that  $\text{CoCl}_2$  mimetic hypoxia induced autophagy in ACC, and the HIF-1 $\alpha$ /BNIP3 signaling pathway was important in the activation of hypoxia-induced autophagy in ACC. Furthermore, inhibition of autophagy suppressed tumor invasion induced by hypoxia. These findings reinforce the importance of autophagy in tumor progression and indicate that manipulation of hypoxia-induced autophagy may offer a novel target for ACC therapy.

## Acknowledgements

The present study was supported by grants from the Shandong Provincial Science and Technology Development Plan (grant no. 2006GG2202034), the Science and Technology Foundation of the Shandong Province (grant no. 2006GG20002046) and the Shandong Provincial Natural Science Foundation (grant no. ZR2012HQ022).

## References

- Adelstein DJ, Koyfman SA, El-Naggar AK and Hanna EY: Biology and management of salivary gland cancers. *Semin Radiat Oncol* 22: 245-253, 2012.
- Dodd RL and Slevin NJ: Salivary gland adenoid cystic carcinoma: A review of chemotherapy and molecular therapies. *Oral Oncol* 42: 759-769, 2006.
- Bradley PJ: Adenoid cystic carcinoma of the head and neck: A review. *Curr Opin Otolaryngol Head Neck Surg* 12: 127-132, 2004.
- Janssen HL, Haustermans KM, Balm AJ and Begg AC: Hypoxia in head and neck cancer: How much, how important? *Head Neck* 27: 622-638, 2005.
- Rouschop KM and Wouters BG: Regulation of autophagy through multiple independent hypoxic signaling pathways. *Curr Mol Med* 9: 417-424, 2009.
- Toustrup K, Sørensen BS, Alsner J and Overgaard J: Hypoxia gene expression signatures as prognostic and predictive markers in head and neck radiotherapy. *Semin Radiat Oncol* 22: 119-127, 2012.
- Adams JM, Difazio LT, Rolandelli RH, Luján JJ, Haskó G, Csóka B, Selmezy Z and Németh ZH: HIF-1: A key mediator in hypoxia. *Acta Physiol Hung* 96: 19-28, 2009.
- Semenza GL: HIF-1 and mechanisms of hypoxia sensing. *Curr Opin Cell Biol* 13: 167-171, 2001.
- Brennan PA, Mackenzie N and Quintero M: Hypoxia-inducible factor 1 $\alpha$  in oral cancer. *J Oral Pathol Med* 34: 385-389, 2005.
- Costa AF, Tasso MG, Mariano FV, Soares AB, Chone CT, Crespo AN, Fresno MF, Llorente JL, Suárez C, de Araújo VC, *et al*: Levels and patterns of expression of hypoxia-inducible factor-1 $\alpha$ , vascular endothelial growth factor, glucose transporter-1 and CD105 in adenoid cystic carcinomas with high-grade transformation. *Histopathology* 60: 816-825, 2012.
- Zhou C, Liu J, Tang Y, Zhu G, Zheng M, Jiang J, Yang J and Liang X: Coexpression of hypoxia-inducible factor-2 $\alpha$ , TWIST2 and SIP1 may correlate with invasion and metastasis of salivary adenoid cystic carcinoma. *J Oral Pathol Med* 41: 424-431, 2012.
- Chen N and Karantza V: Autophagy as a therapeutic target in cancer. *Cancer Biol Ther* 11: 157-168, 2011.
- White E and DiPaola RS: The double-edged sword of autophagy modulation in cancer. *Clin Cancer Res* 15: 5308-5316, 2009.
- Jiang L, Huang S, Li W, Zhang D, Zhang S, Zhang W, Zheng P and Chen Z: Expression of autophagy and ER stress-related proteins in primary salivary adenoid cystic carcinoma. *Pathol Res Pract* 208: 635-641, 2012.
- Jiang L, Huang S, Zhang D, Zhang B, Li K, Li W, Zhang S, Zhang W and Zheng P: Inhibition of autophagy augments chemotherapy in human salivary adenoid cystic carcinoma. *J Oral Pathol Med* 43: 265-272, 2014.
- Ma B, Liang LZ, Liao GQ, Liang YJ, Liu HC, Zheng GS and Su YX: Inhibition of autophagy enhances cisplatin cytotoxicity in human adenoid cystic carcinoma cells of salivary glands. *J Oral Pathol Med* 42: 774-780, 2013.
- Mizushima N and Yoshimori T: How to interpret LC3 immunoblotting. *Autophagy* 3: 542-545, 2007.
- Mazure NM and Pouyssegur J: Hypoxia-induced autophagy: Cell death or cell survival? *Curr Opin Cell Biol* 22: 177-180, 2010.
- Bellot G, Garcia-Medina R, Gounon P, Chiche J, Roux D, Pouyssegur J and Mazure NM: Hypoxia-induced autophagy is mediated through hypoxia-inducible factor induction of BNIP3 and BNIP3L via their BH3 domains. *Mol Cell Biol* 29: 2570-2581, 2009.
- Azad MB and Gibson SB: Role of BNIP3 in proliferation and hypoxia-induced autophagy: Implications for personalized cancer therapies. *Ann N Y Acad Sci* 1210: 8-16, 2010.
- Wang GL and Semenza GL: General involvement of hypoxia-inducible factor 1 in transcriptional response to hypoxia. *Proc Natl Acad Sci USA* 90: 4304-4308, 1993.
- Song ZC, Zhou W, Shu R and Ni J: Hypoxia induces apoptosis and autophagic cell death in human periodontal ligament cells through HIF-1 $\alpha$  pathway. *Cell Prolif* 45: 239-248, 2012.
- Naves T, Jawhari S, Jauberteau MO, Ratinaud MH and Verdier M: Autophagy takes place in mutated p53 neuroblastoma cells in response to hypoxia mimetic  $\text{CoCl}_2$ . *Biochem Pharmacol* 85: 1153-1161, 2013.
- Rovetta F, Stacchiotti A, Faggi F, Catalani S, Apostoli P, Fanzani A and Aleo MF: Cobalt triggers necrotic cell death and atrophy in skeletal C2C12 myotubes. *Toxicol Appl Pharmacol* 271: 196-205, 2013.
- Chinnadurai G, Vijayalingam S and Gibson SB: BNIP3 subfamily BH3-only proteins: Mitochondrial stress sensors in normal and pathological functions. *Oncogene* 27 (Suppl 1): S114-S127, 2008.
- Vengellur A and LaPres JJ: The role of hypoxia inducible factor 1 $\alpha$  in cobalt chloride induced cell death in mouse embryonic fibroblasts. *Toxicol Sci* 82: 638-646, 2004.
- Zhao X, He Y and Chen H: Autophagic tumor stroma: Mechanisms and roles in tumor growth and progression. *Int J Cancer* 132: 1-8, 2013.
- Bohensky J, Shapiro IM, Leshinsky S, Terkhorn SP, Adams CS and Srinivas V: HIF-1 regulation of chondrocyte apoptosis: Induction of the autophagic pathway. *Autophagy* 3: 207-214, 2007.
- Maiuri MC, Le Toumelin G, Criollo A, Rain JC, Gautier F, Juin P, Tasdemir E, Pierron G, Troulinaki K, Tavernarakis N, *et al*: Functional and physical interaction between Bcl-X (L) and a BH3-like domain in Beclin-1. *EMBO J* 26: 2527-2539, 2007.
- Maiuri MC, Criollo A, Tasdemir E, Vicencio JM, Tajeddine N, Hickman JA, Geneste O and Kroemer G: BH3-only proteins and BH3 mimetics induce autophagy by competitively disrupting the interaction between Beclin 1 and Bcl-2/Bcl-X (L). *Autophagy* 3: 374-376, 2007.
- Wouters BG, Weppler SA, Koritzinsky M, Landuyt W, Nuyts S, Theys J, Chiu RK and Lambin P: Hypoxia as a target for combined modality treatments. *Eur J Cancer* 38: 240-257, 2002.
- Macintosh RL, Timpson P, Thorburn J, Anderson KI, Thorburn A and Ryan KM: Inhibition of autophagy impairs tumor cell invasion in an organotypic model. *Cell Cycle* 11: 2022-2029, 2012.

33. Li J, Yang B, Zhou Q, Wu Y, Shang D, Guo Y, Song Z, Zheng Q and Xiong J: Autophagy promotes hepatocellular carcinoma cell invasion through activation of epithelial-mesenchymal transition. *Carcinogenesis* 34: 1343-1351, 2013.
34. Yamanaka-Tatematsu M, Nakashima A, Fujita N, Shima T, Yoshimori T and Saito S: Autophagy Induced by HIF1 $\alpha$  over-expression supports trophoblast invasion by supplying cellular energy. *PloS One* 8: e76605, 2013.
35. Gu BJ and Wiley JS: Rapid ATP-induced release of matrix metalloproteinase 9 is mediated by the P2X7 receptor. *Blood* 107: 4946-4953, 2006.
36. Indelicato M, Pucci B, Schito L, Reali V, Aventaggiato M, Mazzarino MC, Stivala F, Fini M, Russo MA and Tafani M: Role of hypoxia and autophagy in MDA-MB-231 invasiveness. *J Cell Physiol* 223: 359-368, 2010.